

The nanostructure and electrical properties of SWNT bundle networks grown by an ‘all-laser’ growth process for nanoelectronic device applications

M A El Khakani¹ and J H Yi

Institut National de la Recherche Scientifique, INRS-Énergie, Matériaux et Télécommunications, 1650, Boulevard Lionel-Boulet, CP 1020, Varennes, QC, J3X-1S2, Canada

E-mail: elkhakan@inrs-emt.quebec.ca

Received 15 January 2004

Published 23 July 2004

Online at stacks.iop.org/Nano/15/S534

doi:10.1088/0957-4484/15/10/007

Abstract

We report on an ‘all-laser’ synthesis approach that permits the control of the lateral growth of single wall nanotubes (SWNTs) on SiO₂/Si substrates at selected locations where nanoparticles catalysts were first deposited. This novel two-step growth process uses the same UV laser (KrF excimer; $\lambda = 248$ nm) to deposit, in a first step, the CoNi nanoparticle catalysts on patterned SiO₂/Si substrates and, in a subsequent step, to grow the SWNTs. Atomic force microscopy and micro-Raman spectroscopy revealed that the ‘all-laser’ process leads to the formation of horizontal random networks of SWNT bundles, that bridge two adjacent nanoparticle strips. The diameter of the SWNTs was found to be ~ 1.1 nm, while that of the bundles is generally in the 10–15 nm range. The current (I)–voltage (V_{SD}) characteristics of the fabricated SWNT devices confirmed that the random networks of SWNT bundles exhibit a p-type field-effect transistor behaviour. Conductance (G)–gate voltage (V_G) curves not only demonstrated that transport through the bundle networks was dominated by positive carriers (holes) but also that the bundles consist of mixtures of semiconducting and metallic SWNTs. The extremely high efficiency of our ‘all-laser’ growth process in producing high-quality SWNTs together with its relative simplicity definitely open new prospects for the development and integration of novel architectures of nanodevices based on SWNT networks.

(Some figures in this article are in colour only in the electronic version)

1. Introduction

Single wall carbon nanotubes (SWNTs) are known to be ideal building blocks for novel nanoelectronic devices because of their unique electrical properties which depend on their chirality and diameter [1–3]. Their successful use for the development of various nanoscale electronic devices

(such as field effect transistors (FETs), diodes or memories) [4–7] has fostered the R&D in the emerging field of SWNT-based nanodevices. In particular, since they were first made in 1998 [4], FETs made from semiconducting SWNTs are continuing to be the subject of intense investigations mainly because of their outstanding transport properties such as their unprecedented room-temperature mobility that has been very recently reported to be more than 70 times higher than that of standard silicon MOSFETs [8]. The fabrication

¹ Author to whom any correspondence should be addressed.

process of the SWNT-based FETs generally consists of various successive steps starting from the synthesis of the nanotubes, their purification and cleaning, dispersion in a solution and spreading on a substrate to their precise positioning and final connection to metal electrodes [4, 9]. However, such processing is highly laborious and time-consuming, particularly when it comes to the challenging task of the precise positioning of the nanotubes on the substrate and their correct attachment to the metal electrodes. In contrast, few recent works have reported the possibility of fabricating FETs from random arrays of SWNTs [10–12]. The major advantage of this approach is that random arrays of SWNTs can be easily achieved either by direct growth on catalyzed substrates or simply through the spreading of an aqueous suspension of SWNTs onto a substrate. A common feature to these few works reported on the SWNT random networks-based FETs [10–12] is that they have used chemical vapour deposition (CVD) to grow the SWNTs directly on catalyzed substrates. It is worth noting here that the preparation of catalyst nanoparticles on the substrate is a prerequisite for the CVD growth of carbon SWNTs [13–16]. This substrate preparation is a preliminary step that is generally achieved either by chemical processing, such as a controlled impregnation of the substrate by iron nanoparticles [13, 14, 16], or by physically evaporating a sub-monolayer of the metal catalyst on the substrate [14, 16].

In this paper, we propose an ‘all-laser’ synthesis approach for the controlled growth of SWNTs on SiO₂/Si substrates. This novel approach uses the same UV laser to deposit the CoNi catalyst nanoparticles and subsequently to grow the carbon SWNTs. The laser-based synthesis is known to offer the advantage of producing exclusively SWNTs with the highest purity ever reported [17]. Moreover, we have demonstrated for the first time that high-quality SWNTs can also be grown by means of a KrF UV laser at processing temperatures even lower than those required for the most commonly used Nd:YAG lasers [18]. Here, focus is put on both the successful use of our ‘all-laser’ growth process for the integration of SWNT bundle networks into FET-like devices and the investigation of their electrical properties. We were thus able to show that the random networks of SWNT bundles produced by the ‘all-laser’ approach exhibit a p-type semiconducting FET behaviour.

2. Experiment

The ‘all-laser’ process for the fabrication of SWNT bundle-networks-based FETs is summarized in figure 1. This process can be divided into the five following steps:

- (i) UV photolithography patterning to achieve photoresist lines of 2 μm width on 400 nm-thick SiO₂ film thermally grown on Si(100) wafers (figure 1(a));
- (ii) pulsed laser deposition (PLD) of CoNi nanoparticles (figure 1(b));
- (iii) lift-off of the photoresist which leads to SiO₂/Si substrates with CoNi nanoparticle lines separated by a 2 μm gap (figure 1(c));
- (iv) direct UV-laser growth of the SWNTs on the substrates patterned with CoNi catalyst nanoparticles (figure 1(d)); and

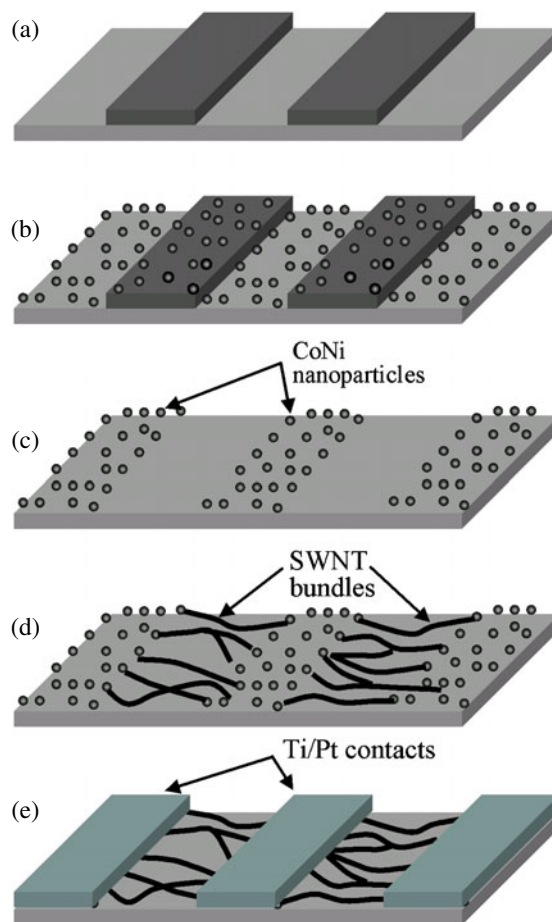


Figure 1. Schematic sequence of the five main steps of the ‘all-laser’ process for the fabrication of SWNT bundle-networks-based devices.

- (v) finally, sputter-deposition of Ti/Pt contact electrodes through a second photolithography patterning and alignment step (figure 1(e)).

The CoNi nanoparticle deposition (figure 1(b)) was achieved by ablating a polycrystalline CoNi target (99.95%) using a KrF excimer laser (wavelength = 248 nm; pulse duration = 15 ns) with an on-target laser intensity of $\sim 4 \times 10^8 \text{ W cm}^{-2}$ under a helium background atmosphere at room temperature. The incident KrF laser beam was focused at an incident angle of 45° onto the CoNi target with a repetition rate of 10 Hz. Since the characteristics of catalyst nanoparticles, such as particle size and surface density, are known to influence strongly their catalytic behaviour for the nanotube growth [19–22], we have chosen the PLD conditions that yield CoNi nanoparticles with diameters of few nanometres. These conditions are a background He pressure of 300 mTorr, a target–substrate distance of 5 cm and a laser pulse number of 100. More details on the PLD of CoNi nanoparticles for use as nucleation sites for the growth of SWNTs were described elsewhere [23]. Figure 2(a) shows a typical atomic force microscopy (AFM) image of the CoNi nanoparticles deposited under the above-mentioned PLD conditions. It is clearly seen that the discrete CoNi nanoparticles are well dispersed on the substrate with a mean diameter of $(2.4 \pm 0.6) \text{ nm}$ (see figure 2(b)) and a surface density of $\sim 4 \times 10^{10} \text{ cm}^{-2}$. It is

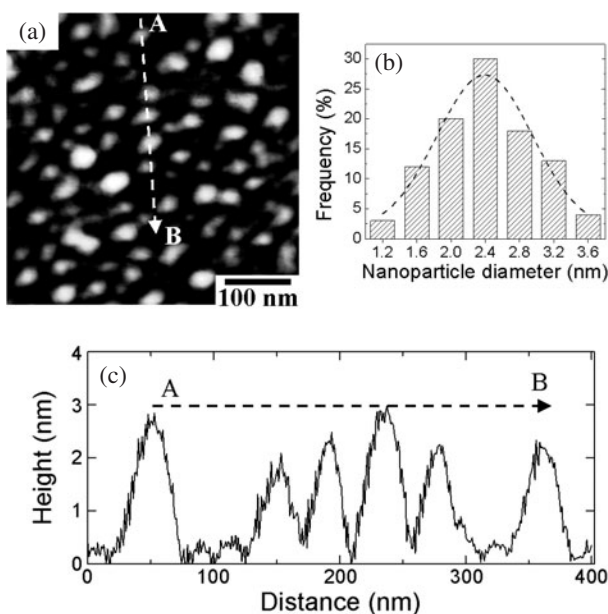


Figure 2. (a) Atomic force microscopy image of the pulsed laser deposited CoNi nanoparticles deposited on a SiO₂/Si surface; (b) size distribution histogram for PLD CoNi nanoparticles used as a catalyst for the SWNT growth; and (c) linescan height profile along the A–B segment in (a).

worth recalling that the particle diameters were measured from their topographic height (figure 2(c)) rather than from their lateral dimension because of the convolution with the AFM tip, the radius of which is much larger than the actual size of the nanoparticles.

The direct growth of SWNTs from the CoNi nanoparticle patterned lines (figure 1(d)) was performed by placing the patterned substrates in the centre of the quartz tube of a furnace. Then the carbon vapour that leads to the growth of SWNTs on the CoNi nanoparticles is provided by the laser ablation of a pure graphite target. The ablation was carried out in argon atmosphere (5 Torr) at various temperatures, in the 800–1200 °C range, with an on-target KrF laser intensity of $\sim 3 \times 10^8$ W cm⁻². This laser intensity has been shown to be optimal for the growth of SWNTs by means of KrF UV lasers [18, 24]. In the present work, the SWNTs were obtained from the ablation of the graphite target by 100 laser shots.

As-deposited CoNi nanoparticles and grown nanotubes were characterized by means of AFM (NanoScope III, Digital Instrument) and/or micro-Raman spectroscopy (Renishaw Imaging Microscope WireTM, $\lambda = 514.5$ nm) in air at room temperature. The transport properties of the fabricated SWNT bundle-networks-based FET devices were investigated by using Ti/Pt electrodes as source and drain and Si substrate as a back gate (as illustrated in figure 5(a)). These devices were characterized at room temperature in air using a Hewlett-Packard 4140B semiconductor parameter analyser.

3. Results and discussion

Figure 3 shows typical AFM images of SiO₂/Si substrate surfaces after the carbon deposition (i.e., the fourth step of the above-described fabrication process) at various furnace temperatures. For the samples prepared at a furnace

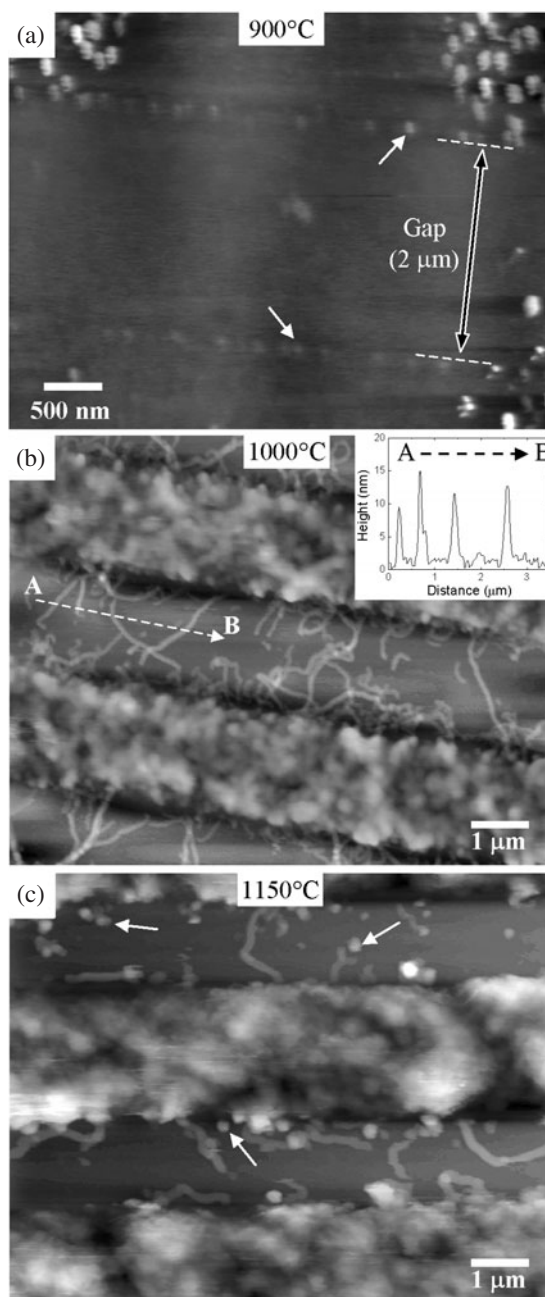


Figure 3. Typical AFM images of patterned SiO₂/Si surfaces after carbon deposition at increasing furnace temperatures: (a) 900 °C, (b) 1000 °C, and (c) 1150 °C. The inset of (b) is a linescan height profile along the A–B line-cut (dashed white line).

temperature of 900 °C, no nanotubes were observed either in the 2 μm gap or on the CoNi strips, and only some particle-like deposits are present on the samples (figure 3(a)). Indeed, the relatively large particles (diameter in the 10–20 nm range) that can be seen at the top left, top right and bottom right corners of figure 3(a) are undoubtedly carbon nanostructures resulting from the laser ablation of the graphite target. One can still distinguish CoNi nanoparticles (~ 2.2 nm-diameter) that are located along the edges of the patterned lines (white arrows in figure 3(a)). The Raman spectrum of figure 4(a) also confirms that there is no evidence for nanotube growth on the sample prepared at 900 °C. These results indicate that the catalytic

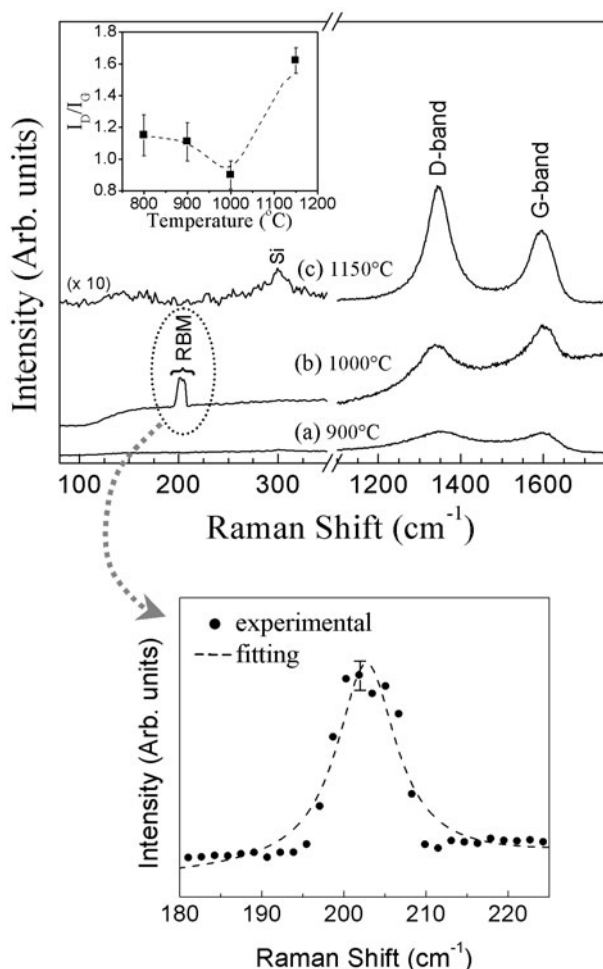


Figure 4. Raman spectra of the SWNT bundle networks produced on SiO₂/Si substrates by using the ‘all-laser’ growth process at different furnace temperatures: (a) 900 °C, (b) 1000 °C, and (c) 1150 °C. The inset shows the variation of the I_D/I_G intensity ratio as a function of the furnace temperature.

effect of the CoNi nanoparticles is not sufficient for nanotube growth at furnace temperatures ≤ 900 °C. In contrast, when the carbon deposition was carried out at 1000 °C, the AFM images (figure 3(b)) clearly revealed the presence of random networks of tubular structures between the CoNi nanoparticle strips. The diameter of more than 50 tubular nanostructures was found to be in the 10–15 nm range (as illustrated by the inset of figure 3(b)), while the corresponding Raman spectrum (figure 4(b)) has revealed the presence of a very sharp radial breathing mode (RBM). This RBM absorption band can be fitted by a single Lorentzian line centred around 203 cm^{-1} with an FWHM of 8.7 cm^{-1} , which is a typical value for the width of phonons in a bundle of SWNTs [25]. This is well illustrated in the zoomed window of the RBM band in the lower panel of figure 4. By using the relation proposed by Bandow *et al* (i.e., d (nm) = 223.75/ ω , where d is the tube diameter and ω is the frequency in cm^{-1}) [26], the diameter of the nanotubes was found to be of (1.1 \pm 0.1) nm. It is worth noting here that ~ 1.1 nm diameter nanotubes can be either metallic, such as armchair (8, 8) tubes [27], or semiconducting, such as chiral (10, 6) and (9, 7) tubes [28]. This confirms that the tubular nanostructures are bundles of SWNTs, which are seen

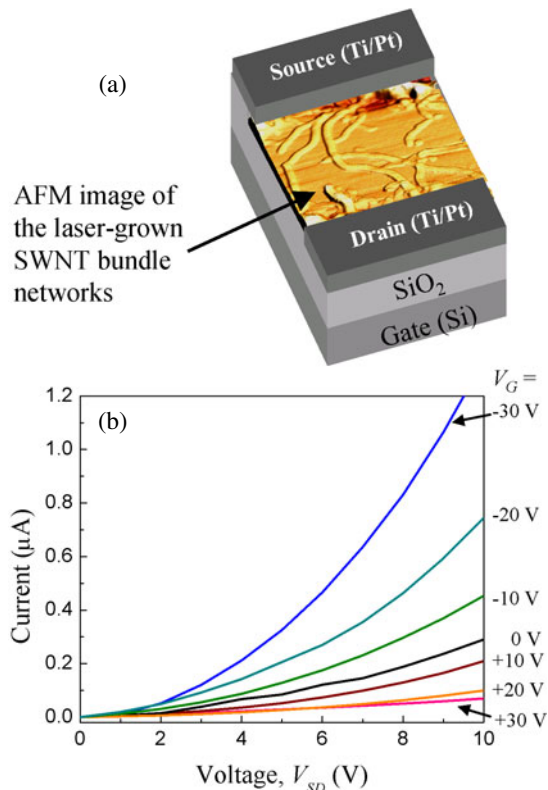


Figure 5. (a) Schematics of the developed SWNT bundle-networks-based FET device; and (b) typical I – V_{SD} characteristics of the device as a function of the gate voltage V_G .

to bridge the 2 μm gap between the CoNi nanoparticle strips. These SWNT bundles are found to grow laterally, forming most often random networks that connect CoNi nanoparticles of two adjacent strips (single bundles directly crossing the gap were also observed). The length of SWNT bundles reached up to several micrometers, and some bundles connected to others through X, Y, and T junctions. Other bundle arrangements such as tree-like branching and loops were also observed. The density of SWNT bundles, defined as the total length (in μm) of the bundles per μm^2 , grown at 1000 °C was estimated to be $\sim 1.5 \mu\text{m}^{-1}$. Such a density value shows that our ‘all-laser’ synthesis process is extremely efficient in converting graphite carbon into SWNTs, particularly when recalling that these SWNTs were obtained by only 100 laser ablation shots of the graphite target. Such a number of laser shots would correspond to an equivalent continuous carbon coverage thickness of only ~ 4 nm.

By increasing the furnace temperature to 1150 °C, surprisingly only a few bundles of SWNTs were formed on the SiO₂/Si surface (figure 3(c)). The density of SWNT bundles was found to decrease considerably to $\sim 0.3 \mu\text{m}^{-1}$ (versus 1.5 μm^{-1} at 1000 °C). This low SWNT growth yield is also confirmed by the very weak RBM absorption band in the corresponding Raman spectrum (figure 4(c)). Moreover, the ratio of the intensities of the D-band to the G-band (I_D/I_G , which is proportional to the relative amount of amorphous carbon or other disordered sp^2 carbon [17]) of the samples grown at 1150 °C, is significantly higher (~ 1.7) than that of those prepared at 1000 °C (~ 0.9). This latter feature correlates with the relatively high quantity of carbon particles (white

arrows in figure 3(c)) observed on the sample prepared at 1150 °C. It should be also noted here that I_D/I_G reaches its minimum value at the furnace temperature of 1000 °C (inset of figure 4), at which the highest SWNT yield is obtained.

In the classical laser synthesis of SWNTs (where a soot containing SWNTs is produced from the ablation of a catalyst-doped graphite target), it is well known that the production yield of SWNTs increases with increasing furnace temperatures up to ~1300 °C and then suddenly decreases around eutectic temperatures (1320 °C for Co–C and 1326 °C for Ni–C) [18, 29]. This tendency was not observed in our ‘all-laser’ process, where the localized growth of SWNTs occurs through the interaction of the ablated carbon vapour with CoNi nanoparticle catalysts on the substrate. The observed decrease of the SWNT yield, when the furnace temperature is increased from 1000 to 1150 °C, is undoubtedly due to the loss of catalytic CoNi nanoparticles, which were found to react with the underlying substrates, leading thereby to the formation of CoSi₂ and NiSi₂ compounds at 1150 °C, as revealed by x-ray diffraction analysis (spectra not shown here). Finally, our results clearly point out the furnace temperature of 1000 °C as the optimal temperature for the localized growth of SWNTs on SiO₂/Si substrates patterned with CoNi nanoparticles.

The laser synthesized SWNT bundle networks were integrated into FET-like devices (as illustrated in figure 5(a)) and their electrical properties were investigated. Figure 5(b) shows the output current–voltage ($I-V_{SD}$) characteristics $I-V_{SD}$ of the SWNT bundles-network-based devices for several values of the gate voltage (V_G). For $V_G = 0$ V, the linear part of the $I-V_{SD}$ curve ($V_{SD} \geq 7$ V) yields a resistance value of ~20 M Ω . For negative V_G values, the slope of the $I-V_{SD}$ curves significantly increases, while it decreases with increasing positive V_G values. This indicates a transition from a conducting to an insulating state of the nanotubes [4]. Nevertheless, even at a negative gate voltage as high as –30 V, the $I-V_{SD}$ curves show a relatively high resistance value (~4 M Ω), which is probably due to the contact resistance R_C between the metal electrodes (Ti/Pt) and the nanotubes. A typical conductance (G)–gate voltage (V_G) curve of the SWNT network-based devices is reported in figure 6. One can easily note that the conductance significantly increases from about 3 nS at $V_G \geq 30$ V to reach ~135 nS for negative V_G values in excess of 30 V, corresponding to an ON/OFF switching ratio of ~45. This behaviour not only demonstrates that transport through the nanotube networks is dominated by positive carriers (holes) but also that the device operates like a field effect transistor. This shows that a random network of SWNT bundles collectively exhibit a FET behaviour similar to that of a single nanotube.

On the other hand, when positive gate voltages were applied, the conductance did not reach the ultimate zero value (i.e., the ideal OFF-state). Indeed, figure 6 shows that the OFF-state of the device is characterized by a low residual G value of ~3 nS for V_G values ≥ 30 V. This result indicates that the SWNT bundle networks are mixtures of semiconducting and metallic SWNTs (in accordance with the above-discussed Raman results). Since the conductance of semiconducting SWNTs is gate-dependent, whereas that of metallic SWNTs is gate-independent [30, 31], the residual G value measured after the depletion of the predominantly p-type semiconducting

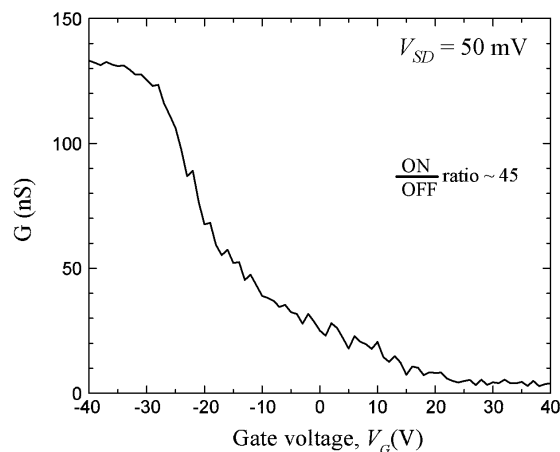


Figure 6. Conductance (G) versus gate voltage (V_G) of the SWNT bundle-network-based device, for a V_{SD} voltage of 50 mV.

SWNTs (by applying high positive V_G) should be attributed to the presence of metallic tubes [30]. To reach the OFF-state of the SWNT bundles-network-based FETs ($G \sim$ zero), it is essential to eliminate the contribution of the metallic SWNTs completely. To this end, the current-induced electrical breakdown method has been shown to be effective, particularly for thin bundles (a few nanometres in diameter), for the selective removal of metallic SWNTs in the bundles [31]. By using this approach, the residual conductance can be reduced by a factor of up to ~3 when applying breakdown voltages of ~80 V. However, since our SWNT bundles are relatively thick (10–15 nm-diameter; this implies a bundle of more than 100 nanotubes), the complete destruction of the metallic nanotubes was found to require high breakdown voltages which generally end up by also destroying the semiconducting tubes. Work is underway to optimize the selective removal of metallic tubes, particularly by targeting the laser growth of thinner SWNT bundles.

4. Conclusion

Direct growth of networks of SWNT bundles on patterned SiO₂/Si has been successfully achieved by means of our newly developed ‘all-laser’ growth process. A furnace temperature of 1000 °C has been identified as the optimal growth temperature that leads to the growth of the highest density of SWNT bundles on the CoNi nanoparticles patterned SiO₂/Si substrates, with the lowest relative amount of amorphous and/or disordered sp² carbon. By integrating the ‘all-laser’ synthesized nanotubes into FET-like devices, we were able to show that the SWNT networks exhibit a p-type semiconducting FET behaviour. Nevertheless, two key issues have still to be addressed in order to improve the electrical characteristics of these devices. These are:

- (i) improving the quality of the nanotube–metal electrode contacts to lower further the contact resistance; and
- (ii) developing strategies to achieve exclusively semiconducting tubes in the bundles.

Finally, in addition to being flexible and relatively easy to implement, the ‘all-laser’ approach is shown to be a very effective tool for the localized growth of SWNTs and their

direct integration into devices with minimum post-processing. This will definitely open up new prospects in the field of laser synthesis of SWNTs and their use for the development of nanoscale devices.

Acknowledgments

This work was financially supported by the Québec Research Network in Nanoscience and Nanotechnology (NanoQuébec) and the Natural Science and Engineering Research Council (NSERC) of Canada.

References

- [1] Baughman R H, Zakhidov A A and Heer W A 2002 *Science* **297** 787
- [2] Terrones M, Terrones H, Banhart F, Charlier J C and Ajayan P M 2000 *Science* **288** 1227
- [3] Dresselhaus M S, Dresselhaus G and Saito R 1992 *Phys. Rev. B* **45** 6234
- [4] Tans S J, Verschueren A R M and Dekker C 1998 *Nature* **393** 49
- [5] Rueckes T, Kim K, Joselevich E, Tseng G Y, Cheung C L and Lieber C M 2000 *Science* **289** 94
- [6] Freitag M, Radosavljevic M, Zhou Y, Johnson A T and Smith W F 2001 *Appl. Phys. Lett.* **79** 3326
- [7] Wind S J, Appenzeller J, Martel R, Derycke V and Avouris Ph 2002 *Appl. Phys. Lett.* **80** 3817
- [8] Durkop T, Getty S A, Cobas E and Fuhrer M S 2004 *Nano Lett.* **4** 35
- [9] Martel R, Schmidt T, Shea H R, Hertel T and Avouris Ph 1998 *Appl. Phys. Lett.* **73** 2447
- [10] Snow E S, Novak J P, Campbell P M and Park D 2003 *Appl. Phys. Lett.* **82** 2145
- [11] Bradley K, Gabriel J C P and Gruner G 2003 *Nano Lett.* **3** 1353
- [12] Marty L, Bouchiat V, Bonnot A M, Chaumont M, Fournier T, Decossas S and Roche S 2002 *Microelectron. Eng.* **61/62** 485
- [13] Kong J, Soh H T, Cassell A M, Quate C F and Dai H 1998 *Nature* **395** 878
- [14] Hongo H, Yudasaka M, Ichihashi T, Nihey F and Iijima S 2002 *Chem. Phys. Lett.* **361** 349
- [15] Moiala A, Nasibulin A G and Kauppinen E 2003 *J. Phys.: Condens. Matter* **15** S3011
- [16] Li Y *et al* 2004 *Nano Lett.* **4** 317
- [17] Braidy N, El Khakani M A and Botton G A 2002 *Carbon* **40** 2835 and references therein
- [18] Braidy N, El Khakani M A and Botton G A 2002 *Chem. Phys. Lett.* **354** 88
- [19] Dai H, Kong J, Zhou C, Franklin N, Tomblor T, Cassell A, Fan S and Chapline M 1999 *J. Phys. Chem. B* **103** 11246
- [20] Li Y, Kim W, Zhang Y, Rolandi M, Wang D and Dai H 2001 *J. Phys. Chem. B* **105** 11424
- [21] Maiti A, Brabec C J and Bernholc J 1997 *Phys. Rev. B* **55** 6097
- [22] Hövel H, Bödecker M, Grimm B and Rettig C 2002 *J. Appl. Phys.* **92** 771
- [23] Yi J H and El Khakani M A 2004 *Nano Lett.* submitted
- [24] Braidy N, El Khakani M A and Botton G A 2002 *J. Mater. Res.* **17** 2189
- [25] Pimenta M A, Marucci A, Brown S D M, Matthews M J, Rao A M, Eklund P C, Smalley R E, Dresselhaus G and Dresselhaus M S 1998 *J. Mater. Res.* **13** 2396
- [26] Bandow S, Asaka S, Saito Y, Rao A M, Grigorian L, Richter E and Eklund P C 1998 *Phys. Rev. Lett.* **80** 3779
- [27] Rao A M *et al* 1997 *Nature* **275** 187
- [28] Jorio A, Saito R, Hafner J H, Lieber C M, Hunter M, McClure T, Dresselhaus G and Dresselhaus M S 2001 *Phys. Rev. Lett.* **86** 1118
- [29] Kataura H, Kumazawa Y, Maniwa Y, Ohtsuka Y, Sen R, Suzuki S and Achiba Y 2000 *Carbon* **38** 1691
- [30] Avouris Ph 2002 *Chem. Phys.* **281** 429
- [31] Collins P G, Arnold M S and Avouris Ph 2001 *Science* **292** 706